

Analytical models of contaminant transport in coastal aquifers

Diogo T. Bolster^{a,*}, Daniel M. Tartakovsky^a, Marco Dentz^b

^a Department of Mechanical and Aerospace Engineering, University of California, San Diego, La Jolla, CA 92093, USA

^b Department of Geotechnical Engineering and Geosciences, Technical University of Catalonia (UPC), Barcelona, Spain

Received 18 November 2006; received in revised form 13 March 2007; accepted 29 March 2007

Available online 14 April 2007

Abstract

The Henry formulation, which couples subsurface flow and salt transport via a variable-density flow formulation, can be used to evaluate the extent of sea water intrusion into coastal aquifers. The coupling gives rise to nontrivial flow patterns that are very different from those observed in inland aquifers. We investigate the influence of these flow patterns on the transport of conservative contaminants in a coastal aquifer. The flow is characterized by two dimensionless parameters: the Péclet number, which compares the relative effects of advective and dispersive transport mechanisms, and a coupling parameter, which describes the importance of the salt water boundary on the flow. We focus our attention on two regimes – low and intermediate Péclet number flows. Two transport scenarios are solved analytically by means of a perturbation analysis. The first, a natural attenuation scenario, describes the flushing of a contaminant from a coastal aquifer by clean fresh water, while the second, a contaminant spill scenario, considers an isolated point source.

© 2007 Elsevier Ltd. All rights reserved.

Keywords: Henry problem; Analytical solution; Seawater intrusion; Variable density flow

1. Introduction

Contamination of freshwater bodies by salt water poses one of the most significant environmental challenges. Within the past few decades, the water quality in many of the coastal aquifers across the world has rapidly degraded. Over-exploitation of the groundwater basins has led to the drops of water tables and seawater intrusion into the aquifers. In many countries, e.g., Cyprus, Mexico, Oman and Israel, hundreds of wells along the coastline had to be shut down. A common source of this salt water is the sea, although naturally occurring brines, landfill leachate and irrigation practices can also result in contamination. The scenario we consider in this study is when sea water intrudes into a coastal aquifer, which poses significant environmental and economical challenges around the world, because even very small proportions of seawater render

freshwater unpotable. Facing a shortage of suitable drinking water, many arid coastal countries have had either to look for alternative sources, such as imported water, or to implement costly technological solutions, such as desalination.

While salt as a source of contamination of coastal aquifers has received considerable attention, other threats to the quality of the groundwater have been studied less systematically. Results from an EU-sponsored project entitled BOREMED (Boron contamination of water resources in the Mediterranean region: distribution, sources, social impact and remediation) show that Boron contamination in coastal aquifers poses a potential threat to the future use of many Mediterranean groundwater basins as a source of drinking and irrigation water [1]. Not only might Boron render potential drinking water unpotable, but it may also make it unsuitable for irrigation since elevated Boron concentrations are known to cause certain crop failure.

Every summer, coastal communities from Maine to California are forced to temporarily close some of their most popular beaches because of unsafe levels of bacteria in the water. Typically, these sudden bacterial blooms disap-

* Corresponding author.

E-mail addresses: dbolster@ucsd.edu, diogobolster@gmail.com (D.T. Bolster), dmt@ucsd.edu (D.M. Tartakovsky), marco.dentz@upc.edu (M. Dentz).

pear, only to return without warning later in the season. In many cases, health officials are unable to pinpoint the cause of the contamination, leading frustrated beachgoers to blame everything from inadequate sewage treatment plants to overwhelmed storm drain systems, while ignoring the possibility of groundwater contamination in the beach aquifer itself. The studies by Boehm et al. [2,3] indicate that a large fraction of this contamination may actually be coming from coastal groundwater.

Across the world, in coastal regions with heavy mining communities, deterioration of coastal aquifers is reaching serious proportions and their viability is currently threatened. For example, according to the Minister of Water Affairs and Forestry of South Africa, the Cape Flats aquifer, a part of the important coastal aquifer system in South Africa, which underlies large mining developments, fits into this category of rapidly deteriorating water sources. These are but a few examples. Others include contamination by heavy metals, groundwater nutrients, fertilizers, etc.

Modeling of contaminant transport in coastal aquifers is complicated by the influence of an intruding seawater wedge on the velocity field within the aquifer. Increased salinity at the seaward boundary distorts the velocity field from a simple cross-flow and introduces vertical velocities along with velocity gradients. Regardless of application, there is a scarcity of analytical solutions to advective-dispersion equation with a variable velocity fields. Such solutions are mostly limited to either steady-state transport or simplified flow conditions or both (e.g., [4]).

For seawater intrusion, the velocity fields can be computed with two alternative paradigms. The first postulates the existence of a sharp interface separating the fresh and salt water. This assumption allows the use of potential theory to derive analytical solutions for the location of this interface (e.g., [5–8]). Since the sharp interface paradigm ignores a transition zone between the fresh and salt water, these and other similar results are strictly valid for advection-dominated systems.

The second paradigm explicitly accounts for the existence of a transitional zone. The model consists of a variable density (Darcy) flow equation coupled with the advection-diffusion equation for the transport of salt. Even for the simplest geometries of a flow domain, this coupling makes it difficult to obtain analytical solutions, which are essential for the testing and validation of numerical codes. To the best of our knowledge, the Henry [9] formulation of variable density flow in coastal aquifers provides the only mathematical setting for which analytical solutions are available. Consequently, Henry's problem is one of the most widely used benchmarking problems. Henry's quasi-analytical solution to this problem is based on a Galerkin projection and results in infinite series, whose slow convergence rates require the extensive use of numerics. Numerical errors that are inherent in these computations might compromise the usefulness of Henry's solution for benchmarking.

Simpson and Clement [10] hypothesized that under certain conditions the Henry problem can be simplified by

replacing the full coupling of the governing equations with a pseudo-coupling that is applied via the boundary conditions (i.e. by assuming that the spatial variability of the water density has negligible effect). Dentz et al. [11] tested this hypothesis by deriving perturbation-based analytical solutions for the fully and pseudo-coupled systems and testing their accuracy and robustness numerically. They showed that for many cases it is indeed sufficient to only implement the coupling via the boundary conditions, which is the approach we adopt in this study.

In this paper, we are concerned with the transport of passive contaminants in a coastal aquifer. The problem is formulated in Section 2 and its dimensional analysis is presented in Section 3. Sections 4 and 5 contain the analyses of two different contamination scenarios corresponding to natural attenuation and isolated sources, respectively.

2. Formulation of Henry problem for contaminant transport

Consider flow and contaminant transport in a confined coastal aquifer in which the diffused seawater wedge is in equilibrium with the freshwater flow field (Fig. 1a). The aquifer is also assumed to be homogeneous and isotropic, with constant hydraulic conductivity and porosity. Following Henry [9], we idealize this problem by treating the flow domain as a rectangle shown in Fig. 1b.

Henry's formulation of the corresponding two-dimensional flow problem is based on mass conservation and a modified Darcy equation written in terms of freshwater head $h(\mathbf{x})$

$$\nabla \cdot \mathbf{q} = 0, \quad \mathbf{q} = -K\nabla \left(h + y\epsilon \frac{c}{c_s} \right), \quad \epsilon \equiv \frac{\rho_s - \rho_f}{\rho_f}, \quad (1)$$

where \mathbf{q} is the fluid flux; K is the hydraulic conductivity; c and c_s are the concentrations of salt in groundwater and sea water, respectively; and ρ_f and ρ_s are the fresh and sea water densities, respectively. The equivalent freshwater head h is defined as

$$h = \frac{p}{\rho_f g} + y, \quad (2)$$

where p is water pressure, g is the gravitational acceleration constant, and y is the vertical coordinate. These equations are subject to the boundary conditions

$$h(x=0, y) = h_0, \quad h(x=L, y) = d + \epsilon(d-y) \quad (3)$$

$$\begin{aligned} \frac{\partial h}{\partial y}(x, y=0) &= -\epsilon \frac{c(x, y=0)}{c_s}, \\ \frac{\partial h}{\partial y}(x, y=d) &= -\epsilon \frac{c(x, y=d)}{c_s}. \end{aligned} \quad (4)$$

The concentration of salt in groundwater, $c(\mathbf{x})$, satisfies a steady advection-diffusion equation

$$K\nabla h \cdot \nabla c + K \frac{c}{c_s} \frac{\partial c}{\partial y} + \omega D \nabla^2 c = 0, \quad (5)$$

where ω is the porosity of the medium and D is the effective (average) dispersion coefficient for salt which, in Henry's

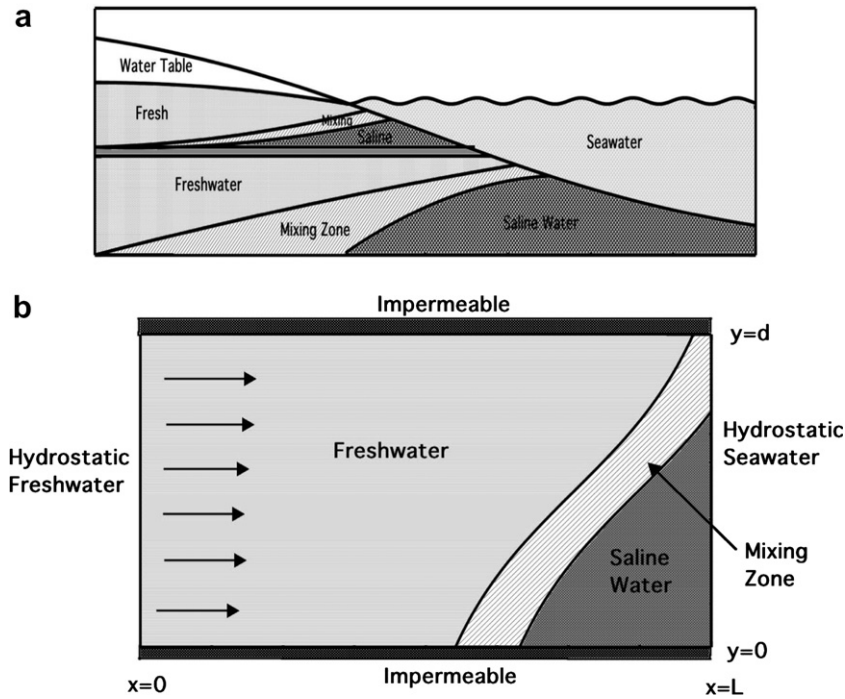


Fig. 1. (a) A schematic representation of a coastal aquifer system and (b) its mathematical conceptualization by Henry [9].

formulation, is assumed to be constant throughout the entire domain. The boundary conditions for salt transport are freshwater at the inlet boundary, saline water at the outlet boundary and impermeable conditions on the top and bottom of the aquifer. This corresponds to

$$c(x=0, y) = 0, \quad c(x=L, y) = c_s, \quad (6)$$

$$\frac{\partial c}{\partial y}(x, y=0) = 0, \quad \frac{\partial c}{\partial y}(x, y=d) = 0. \quad (7)$$

Additionally, consider the migration of a conservative contaminant in the velocity field $\mathbf{u} = \mathbf{q}/\omega$ given by a solution of the Henry problem (1)–(5). The concentration of this contaminant, $\gamma(\mathbf{x}, t)$, satisfies a transient advection-diffusion equation

$$\frac{\partial \gamma}{\partial t} + \mathbf{u} \cdot \nabla \gamma = D_L \frac{\partial^2 \gamma}{\partial x^2} + D_T \frac{\partial^2 \gamma}{\partial y^2}. \quad (8)$$

In the spirit of Henry's formulation, the longitudinal (D_L) and transverse (D_T) dispersion coefficients are assumed to be constant. Kalejaiye and Cardoso [12] showed that this is a legitimate assumption for flows where the Rayleigh number is less than 1000, which holds for all models presented in this paper. We formally define this Rayleigh number, Ra , in the following section on dimensionless analysis. Introducing $D_\gamma \equiv D_L$ and $D_T = \beta D_\gamma$, we rewrite (8) as

$$\frac{\partial \gamma}{\partial t} + \mathbf{u} \cdot \nabla \gamma = D_\gamma \left(\frac{\partial^2 \gamma}{\partial x^2} + \beta \frac{\partial^2 \gamma}{\partial y^2} \right). \quad (9)$$

Depending on a pollutant, D_γ might or might not coincide with the dispersion coefficient for salt, D . To simplify the subsequent presentation, we assume that these two dispersion coefficients are of the same order, $D_\gamma \sim \mathcal{O}(D)$. The specification of initial and boundary conditions for (8) describes a particular contamination scenario, among which we consider two.

The first represents natural attenuation of a contaminated coastal aquifer, a setting in which seaward flow of fresh water flushes out a contaminant that is initially distributed uniformly throughout an aquifer. In addition to its practical significance, this problem allows one to identify regions where contamination is most persistent and to elucidate the effects of seawater intrusion on contaminant transport in coastal aquifers. In particular, our analysis can be used to address important logistical questions, such as: How does the sea boundary affect the clean up process? What are the long-term consequences of contamination? How does contaminant fate and migration in coastal aquifers differ from those in inland confined aquifers?

The second scenario models the spread of a contaminant released from an isolated spill conceptualized here as a point source. Common examples include contaminants leaking from a septic tank, a leak from a pipe or a small spill pool. Due to the linearity of the transport equation, understanding the problem associated with a single source is equivalent to understanding that of any number of point and/or distributed sources.

3. Dimensional analysis

Following [11], we introduce dimensionless parameters

$$\xi = \frac{x}{L}, \quad \eta = \frac{y}{L}, \quad \zeta = \frac{d}{L}, \quad \tau = \frac{\kappa \Delta h_0}{L^2} t, \quad (10)$$

$$C = \frac{c}{c_s}, \quad \Gamma = \frac{\gamma}{\gamma_0}, \quad (10)$$

$$H = \frac{h-d}{\Delta h_0}, \quad \mathbf{U} = \frac{\mathbf{u}L}{K\Delta h_0}, \quad Pe = \frac{K\Delta h_0}{\theta D},$$

$$Pe_\gamma = \frac{K\Delta h_0}{\theta D_\gamma}, \quad \alpha = \frac{\epsilon L}{\Delta h_0} \quad (11)$$

where γ_0 is a problem specific reference contaminant concentration. The governing Eqs. (1)–(8) are recast in the dimensionless form

$$\nabla^2 H = -\alpha \frac{\partial C}{\partial \eta}, \quad \mathbf{U} = -\nabla H - \mathbf{e}_3 \alpha C, \quad (12)$$

$$\nabla H \cdot \nabla C + \alpha C \frac{\partial C}{\partial \xi} + \frac{1}{Pe} \nabla^2 C = 0, \quad (13)$$

and

$$\frac{\partial \Gamma}{\partial \tau} + \mathbf{u} \cdot \nabla \Gamma = \frac{1}{Pe_\gamma} \left(\frac{\partial^2 \Gamma}{\partial \xi^2} + \beta \frac{\partial^2 \Gamma}{\partial \eta^2} \right). \quad (14)$$

The gradients in (12) and (13) are nondimensional (i.e. $\nabla = [\frac{\partial}{\partial \xi}, \frac{\partial}{\partial \eta}]$) as are all gradients from here on in. These equations are subject to the boundary conditions

$$H(0, \eta) = 1, \quad H(1, \eta) = \alpha(\zeta - \eta), \quad (15)$$

and

$$\frac{\partial H}{\partial \eta}(\xi, 0) = -\alpha C(\xi, 0), \quad \frac{\partial H}{\partial \eta}(\xi, 0) = -\alpha C(\xi, 0). \quad (16)$$

It now becomes apparent that flow and transport are governed by three dimensionless parameters Pe , Pe_γ , and α . The Péclet numbers Pe and Pe_γ compare the relative importance of advection and dispersion mechanisms for the transport of salt and contaminant, respectively. The coupling parameter α accounts for density variation between the seawater and fresh water and quantifies the effects of gravity and the salt water boundary on the flow field. Specifically, $\alpha = 0$ corresponds to a uniform horizontal flow; as α increases, gravity effects introduce vertical velocities and modify horizontal ones. The Rayleigh number as defined by [12] is the product of α and Pe (i.e. $Ra = \alpha Pe$).

Contaminant transport under the high Péclet number regimes is dominated by advection. Since diffusion is negligible, contaminant is carried along the flow streamlines, so that its migration is described by solutions to the flow problem. Our analysis deals with the remaining two Péclet number regimes: low and intermediate. Since typical Péclet numbers for coastal aquifers fall within the range $\mathcal{O}(10^{-2}) \leq Pe \leq \mathcal{O}(10^5)$ (Nishikawa of USGS, personal communication), these two Péclet number regimes are of practical significance.

4. Natural attenuation of contaminated coastal aquifers

Consider the following simplified problem of natural attenuation of coastal aquifers. Suppose that at time

$t = 0$ an aquifer is uniformly contaminated by, say, industrial or agricultural pollutants, whose concentration is γ_{in} . Then the sources of contamination are eliminated, and fresh water flowing towards the sea begins to remove the contaminants from the aquifer.

An analytical solution for this idealized scenario, which is based on the assumption that the contaminant is distributed uniformly throughout the aquifer, can be used as a benchmark for numerical analyses of more realistic natural attenuation scenarios. Additionally, the technique of allowing a uniformly distributed contaminant to be drained from the ambient environment – the so-called “step down” method – is routinely used to understand the fundamental physics of the transport phenomenon [13,14].

Our goal is to describe the seaward migration of contaminants and to identify regions where the contamination remains persistent. For this case the reference density defined in the nondimensionalisation in (10) is $\gamma_0 = \gamma_{in}$. Contaminant transport is described by (14) subject to the initial and boundary conditions

$$\Gamma(\xi, \eta, 0) = 1, \quad \frac{\partial \Gamma}{\partial \eta}(\xi, 0, \tau) = \frac{\partial \Gamma}{\partial \eta}(\xi, \zeta, \tau) = 0, \quad (17)$$

$$\Gamma(0, \eta, \tau) = \Gamma(1, \eta, \tau) = 0.$$

The last boundary condition implies that the sea acts as an infinite reservoir that dilutes and immediately carries off the contaminant.

4.1. Intermediate Péclet number

The velocity distribution \mathbf{U} in (14) can be obtained analytically via a perturbation expansion of hydraulic head H and other system states in the coupling parameter α [11]

$$H^{IP}(\xi) = \sum_{k=0}^{\infty} \alpha^k H_k^{IP}(\xi), \quad \mathbf{U}^{IP}(\xi) = \sum_{k=0}^{\infty} \alpha^k \mathbf{U}_k^{IP}(\xi). \quad (18)$$

The convergence of these series requires that α be small, an assumption whose validity is discussed in [11]. If one further assumes that the pseudo-coupled model is valid as well, then the terms in the expansion (18) are

$$H_0^{IP} = 1 - \xi, \quad H_1^{IP} = \eta_B(\xi), \quad H_i^{IP} \equiv 0. \quad (19)$$

where

$$\eta_B = \frac{\xi\zeta}{2} + \sum_{l=1}^{\infty} a_l \cos\left(\frac{l\pi\eta}{\zeta}\right) \frac{\sinh(l\pi\xi/\zeta)}{\sinh(l\pi/\zeta)} \quad \text{and}$$

$$a_l = 2\zeta \frac{1 - (-1)^l}{l^2 \pi^2}. \quad (20)$$

It is worthwhile to recall that the second assumption implies that flow and salt transport are coupled only through the boundary conditions. The numerical and analytical studies [10,11] demonstrated that this assumption remains accurate over a wide range of flow conditions.

Substituting (19)–(20) into (12) and (18), we obtain a solution for the velocity field $\mathbf{U} = (U, V)^T$

$$U_0^{IP} = 1, \quad U_1^{IP} = \frac{\zeta}{2} - \sum_{l=1}^{\infty} l\pi a_l \cos\left(\frac{l\pi\eta}{\zeta}\right) \frac{\cosh(l\pi\zeta/\zeta)}{\sinh(l\pi/\zeta)}, \quad (21)$$

and

$$V_0^{IP} = 0, \quad V_1^{IP} = \sum_{l=1}^{\infty} l\pi a_l \sin\left(\frac{l\pi\eta}{\zeta}\right) \frac{\sinh(l\pi\zeta/\zeta)}{\sinh(l\pi/\zeta)}. \quad (22)$$

Both $U_i^{IP} \equiv 0$ and $V_i^{IP} \equiv 0$ for $i \geq 2$. In analogy to (18), we look for a solution of the contaminant transport problem (14) and (17) in the form of an infinite series in the powers of α ,

$$\Gamma^{IP} = \sum_{k=0}^{\infty} \alpha^k \Gamma_k^{IP}. \quad (23)$$

The leading term in this expansion satisfies

$$\frac{\partial \Gamma_0^{IP}}{\partial \tau} + \frac{\partial \Gamma_0^{IP}}{\partial \xi} = \frac{1}{Pe_\gamma} \left(\frac{\partial^2 \Gamma_0^{IP}}{\partial \xi^2} + \beta \frac{\partial^2 \Gamma_0^{IP}}{\partial \eta^2} \right) \quad (24)$$

subject to initial condition $\Gamma_0^{IP}(x, y, t = 0) = 1$ and the boundary conditions (17). The corresponding solution is

$$\Gamma_0^{IP} = 8\pi e^{\frac{Pe}{2}(\xi - \frac{1}{2})} \sum_{n=0}^{\infty} a_n \sin(n\pi\xi) e^{-\frac{\pi^2 n^2 t}{Pe}}, \quad a_n = n \frac{1 - (-1)^n e^{-Pe/2}}{Pe^2 + 4n^2 \pi^2}. \quad (25)$$

The first-order term Γ_1^{IP} in the expansion (23) satisfies

$$\frac{\partial \Gamma_1^{IP}}{\partial \tau} + \frac{\partial \Gamma_1^{IP}}{\partial \xi} = \frac{1}{Pe_\gamma} \left(\frac{\partial^2 \Gamma_1^{IP}}{\partial \xi^2} + \beta \frac{\partial^2 \Gamma_1^{IP}}{\partial \eta^2} \right) - U_1^{IP} \frac{\partial \Gamma_0^{IP}}{\partial \xi} \quad (26)$$

subject to the homogeneous initial and boundary conditions. A coordinate transformation

$$\hat{\eta} = \eta / \sqrt{\beta} \quad (27)$$

maps (26) onto an isotropic advection–diffusion equation

$$\frac{\partial \Gamma_1^{IP}}{\partial \tau} + \frac{\partial \Gamma_1^{IP}}{\partial \xi} = \frac{1}{Pe_\gamma} \left(\frac{\partial^2 \Gamma_1^{IP}}{\partial \xi^2} + \frac{\partial^2 \Gamma_1^{IP}}{\partial \hat{\eta}^2} \right) - U_1^{IP}(\xi, \hat{\eta}) \frac{\partial \Gamma_0^{IP}}{\partial \xi}. \quad (28)$$

Let

$$G(x, y; \xi, \zeta; \tau) = \frac{4}{\zeta} \left[\sum_{p=1}^{\infty} \sin(p\pi x) \sin(p\pi \xi) \exp\left(-\frac{\pi^2 p^2}{Pe} \tau\right) \right] \times \left[\frac{1}{2} + \sum_{m=1}^{\infty} \cos\left(\frac{m\pi y}{\zeta}\right) \cos\left(\frac{m\pi \eta}{\zeta}\right) \right] \times \exp\left(-\frac{\pi^2 m^2}{Pe \zeta^2} \tau\right) \quad (29)$$

denote the Greens function for an isotropic diffusion equation subject to the appropriate homogeneous initial and boundary conditions. Then a solution of (28) can be written as

$$\Gamma_1^{IP} = - \int_0^\tau \int_0^1 \int_0^{\hat{\zeta}} G(\xi, \hat{\eta}, \zeta_1, \hat{\eta}_1, \tau - t) U_1^{IP}(\xi_1, \hat{\eta}_1) \times \frac{\partial \Gamma_0^{IP}(\xi_1, \hat{\eta}_1, t)}{\partial \xi} e^{-\frac{Pe}{2}(\xi_1 - \frac{1}{2})} d\hat{\eta}_1 d\zeta_1 dt, \quad (30)$$

which can be written in the original coordinate system (ξ, η) as

$$\Gamma_1^{IP} = - \int_0^\tau \int_0^1 \int_0^{\hat{\zeta}} G(\xi, \eta, \zeta_1, \hat{\eta}_1, \tau - t) U_1^{IP}(\xi_1, \hat{\eta}_1) \times \frac{\partial \Gamma_0^{IP}(\xi_1, \hat{\eta}_1, t)}{\partial \xi} e^{-\frac{Pe}{2}(\xi_1 - \frac{1}{2})} d\hat{\eta}_1 d\zeta_1 dt. \quad (31)$$

This solution can be evaluated either analytically or numerically. The former approach consists of evaluating the quadratures analytically and is given in terms of infinite series. These series converge at least exponentially, and hence can be truncated after a few terms. (We do not reproduce this expression here due to its length.) The numerical evaluation consists of computing the quadratures with an adaptive recursive Simpson’s method. Both methods produced identical results and required approximately the same computational time.

To validate the proposed approach and to test its accuracy, we compare the first-order perturbation solution $\Gamma^{IP} \approx \Gamma_0^{IP} + \alpha \Gamma_1^{IP}$ with a numerical (finite difference) solution of the contaminant transport problem (14) and (17). Fig. 2 displays this comparison for $Pe = 10$ and two values of α , (a) $\alpha = 0.5$ and (b) $\alpha = 1$. The two solutions agree very well for the $\alpha = 0.5$ case. The agreement is still good for $\alpha = 1$, although small differences between the perturbation and numerical solutions are more evident.

The effects of the coupling parameter α on contaminant transport are elucidated in Fig. 3, which shows concentration profiles for $Pe = 10$, $\beta = 1$, and several values of α . We also considered different values of $\beta = D_T/D_L \in [0.1, 1]$ and found their effects on contaminant distributions to be negligible. This is because the vertical component of the concentration gradient in this transport regime is very small.

The effects of the coupling parameter α are strongest in the region adjacent to the sea, and diminish further inland. The increase in α leads to a redistribution of contaminant relative to the case where no seawater intrusion occurs. The contaminant concentration is highest in the upper coastal side of the domain and decreases slightly in the lower right part. This behavior is due to the fact that the region of outflow is diminished because of the presence of the intruding sea water. (It does not imply that the contaminant concentration increases as it approaches the seaward boundary.) Similarly, less contaminant is present in the lower right region, because uncontaminated seawater enters and flushes this region. This has important implications for the fate of a contaminant, as discussed in detail in Section 5.

4.2. Small Péclet number

Small Péclet numbers correspond to either high dispersion or small mass fluxes. Both scenarios can occur in coastal aquifers, in which tidal fluctuations increase the effective dispersion coefficients and natural hydraulic gradients are small. Analytical solutions to the flow problem can

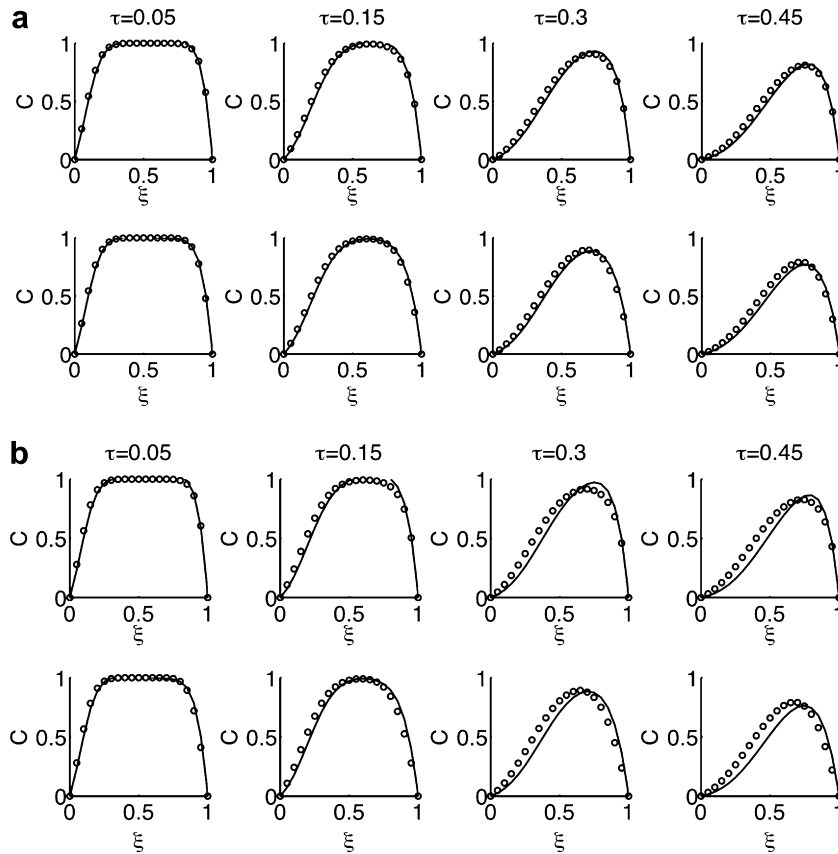


Fig. 2. Temporal snapshots of contaminant concentration distributions of the natural attenuation problem with $Pe = 10$ and (a) $\alpha = 0.5$, (b) $\alpha = 1$ at two heights ($\eta = 0.1$ (top row) and $\eta = 0.4$ (bottom row)) across the width of the aquifer provided by the perturbation (solid line) and numerical (dots) solutions.

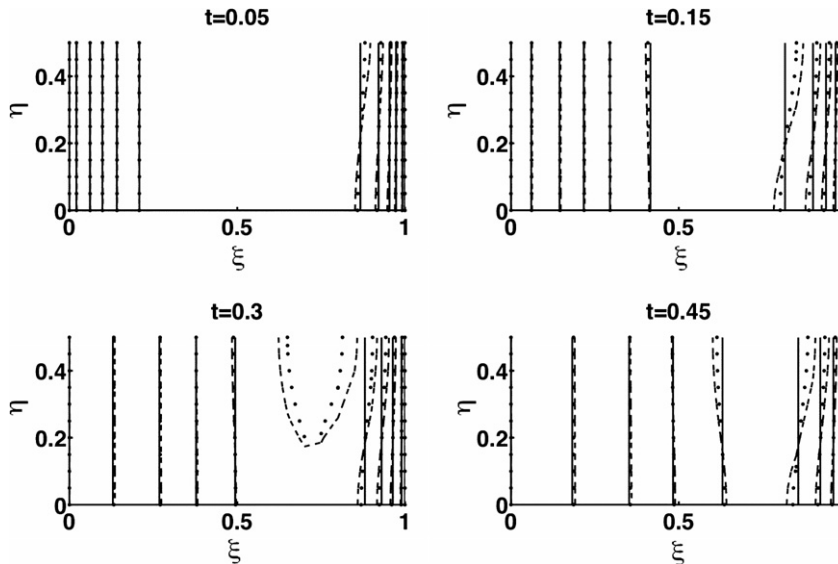


Fig. 3. Temporal snapshots of contaminant concentration distributions provided by the perturbation (solid line) solution of the natural attenuation problem with $Pe = 10$ and $\alpha = 0$ (solid lines), $\alpha = 0.5$ (dots) and $\alpha = 1$ (dashed lines).

now be obtained via perturbation expansions in small Pe [11]

$$H^{SP} = \sum_{n=0}^{\infty} Pe^n H_n^{SP}, \quad \mathbf{U}^{SP} = \sum_{n=0}^{\infty} Pe^n \mathbf{U}_n^{SP}. \quad (32)$$

The leading terms in these expansions are given by

$$H_0^{SP} = 1 - \xi + \alpha \xi (\xi - \eta), \quad \mathbf{U}_0^{SP} = U_0^{SP}(\eta) \mathbf{e}_\xi \equiv [1 + \alpha(\eta - \xi)] \mathbf{e}_\xi, \quad (33)$$

where \mathbf{e}_ξ is the unit vector along the ξ -axis of the coordinate system. Inserting (33) into (14) and rescaling time with the diffusive timescale $t = \tau L/D_\gamma$, we obtain an equation

$$\frac{\partial \Gamma}{\partial \tau} + Pe U_0^{SP}(\eta) \frac{\partial \Gamma}{\partial \xi} - \left(\frac{\partial^2 \Gamma}{\partial \xi^2} + \beta \frac{\partial^2 \Gamma}{\partial \eta^2} \right) = 0, \tag{34}$$

which describes contaminant transport in linear shear flow.

We look for a solution of the transport Eq. (34) subject to the initial and boundary conditions (17) in the form of an infinite series in the powers of Pe

$$\Gamma^{SP} = \sum_{k=0}^{\infty} Pe^k \Gamma_k^{SP}. \tag{35}$$

The leading term in this expansion satisfies

$$\frac{\partial \Gamma_0^{SP}}{\partial \tau} = \frac{\partial^2 \Gamma_0^{SP}}{\partial \xi^2} + \beta \frac{\partial^2 \Gamma_0^{SP}}{\partial \eta^2} \tag{36}$$

subject to initial condition $\Gamma_0^{SP}(\xi, \eta, \tau = 0) = 1$ and the boundary conditions (17). The corresponding solution is

$$\Gamma_0^{SP} = 2 \sum_{n=1}^{\infty} \left[\frac{1 - (-1)^n}{n\pi} \right] \sin(n\pi\xi) e^{-\pi^2 n^2 \tau}. \tag{37}$$

The first-order term in the expansion (35) satisfies

$$\frac{\partial \Gamma_1^{SP}}{\partial \tau} = \frac{\partial^2 \Gamma_1^{SP}}{\partial \xi^2} + \beta \frac{\partial^2 \Gamma_1^{SP}}{\partial \eta^2} - U_0^{SP} \frac{\partial \Gamma_0^{SP}}{\partial \xi} \tag{38}$$

subject to the homogeneous initial and boundary conditions. Using the coordinate transformation (27), we obtain a solution of this equation,

$$\begin{aligned} \Gamma_1^{SP} = & - \int_0^\tau \int_0^1 \int_0^{\hat{\xi}} G(\hat{\xi}, \hat{\eta}; \xi_1, \hat{\eta}_1; \tau - t) U_0^{SP}(\hat{\eta}_1) \\ & \times \frac{\partial \Gamma_0^{SP}(\xi_1, \hat{\eta}_1, \tau)}{\partial x} d\hat{\eta}_1 d\xi_1 dt. \end{aligned} \tag{39}$$

Fig. 4 shows a good agreement between the first-order perturbation solution $\Gamma^{SP} \approx \Gamma_0^{SP} + Pe \Gamma_1^{SP}$ and a finite difference solution of the contaminant transport problem (14) and (17) with $Pe = 0.5$, $\beta = 1$ and $\alpha = 2$. A careful examination of the solution reveals that concentration isolines within the flow domain are slightly tilted, which is a result of the shear flow (33). For $\alpha = 2$ the first-order correction is small, and so is the influence of the sea boundary.

Fig. 5 demonstrates the effects of the coupling parameter α on contaminant transport with $Pe = 0.5$ and $\beta = 1$. Similar to the intermediate Péclet number regime, we found that β has a minimal effect as the dominant direction of transport is in the longitudinal direction. The effects of the saltwater boundary are quite insignificant, with the difference between the solutions corresponding to $\alpha = 0$ and $\alpha = 4$ being minute. At $\alpha = 20$ one can see some tilting of the isolines, but even so it is not all that significant. The relatively small influence of the sea boundary (as quantified by the coupling parameter α large) on contaminant transport process can be explained the fact that, for small Péclet numbers, transport is dominated by diffusion. Since the sea

boundary influences the velocity field and, thus, advective transport, its overall effects on the small-Péclet-number transport is insignificant.

5. Point-source contamination of coastal aquifers

Consider the migration of a pollutant introduced into an initially uncontaminated coastal aquifer by an isolated point source of unit strength (a delta function) located at a point (ξ', η') . This problem, which corresponds to a leak from a storage tank or a pipe, a small spill pool, etc., is described by

$$\frac{\partial \Gamma}{\partial \tau} + \mathbf{U} \cdot \nabla \Gamma = \frac{1}{Pe_\gamma} \nabla^2 \Gamma + \delta(\xi - \xi') \delta(\eta - \eta') \tag{40}$$

subject to the initial and boundary conditions

$$\begin{aligned} \Gamma(\xi, \eta, 0) = 0, \quad \frac{\partial \Gamma}{\partial \eta}(\xi, 0, \tau) = \frac{\partial \Gamma}{\partial \eta}(\xi, \zeta, \tau) = 0, \\ \Gamma(0, \eta, \tau) = \Gamma(1, \eta, \tau) = 0. \end{aligned} \tag{41}$$

Depending on the flow regime, the velocity \mathbf{U} is given by either (21), (22) or (33). Note that due to the linearity of the transport Eq. (40), the solutions obtained in this section can be utilized—by means of a superposition—to describe contaminant migration from multiple point and/or distributed sources.

5.1. Intermediate Péclet number

We represent a solution of the contaminant transport problem (40)-(41) as an infinite series in the powers of α (23). The leading term in this expansion satisfies

$$\frac{\partial \Gamma_0^{IP}}{\partial \tau} + U_0^{IP} \frac{\partial \Gamma_0^{IP}}{\partial \xi} = \frac{1}{Pe} \left(\frac{\partial^2 \Gamma_0^{IP}}{\partial \xi^2} + \beta \frac{\partial^2 \Gamma_0^{IP}}{\partial \eta^2} \right) + \delta(\xi - \xi') \delta(\eta - \eta') \tag{42}$$

subject to the initial and boundary conditions (41). The corresponding solution is

$$\begin{aligned} \Gamma_0^{IP} = & \frac{2}{\hat{\xi}} e^{Pe(\xi - \xi')/2} \sum_{n=1}^{\infty} \frac{\sin(n\pi\xi) \sin(n\pi\xi')}{Pe/4 + \pi^2 n^2 / Pe} \\ & \times \left[1 - e^{-(Pe/4 + \pi^2 n^2 / Pe)t} \right] + \frac{4}{\hat{\xi}} e^{Pe(\xi - \xi')/2} \\ & \times \sum_{n,m=1}^{\infty} \frac{\sin(n\pi\xi) \sin(n\pi\xi') \cos(m\pi\eta/\zeta) \cos(m\pi\eta'/\zeta)}{Pe/4 + \pi^2(n^2 + m^2/\zeta^2)/Pe} \\ & \times \left[1 - e^{-(\frac{Pe}{4} + \frac{\pi^2(n^2 + m^2/\zeta^2)}{Pe})t} \right]. \end{aligned} \tag{43}$$

The first-order term satisfies

$$\frac{\partial \Gamma_1^{IP}}{\partial \tau} + \frac{\partial \Gamma_1^{IP}}{\partial \xi} = \frac{1}{Pe} \left(\frac{\partial^2 \Gamma_1^{IP}}{\partial \xi^2} + \beta \frac{\partial^2 \Gamma_1^{IP}}{\partial \eta^2} \right) - U_1^{IP} \frac{\partial \Gamma_0^{IP}}{\partial \xi} - V_1^{IP} \frac{\partial \Gamma_0^{IP}}{\partial \eta} \tag{44}$$

subject to the initial and boundary conditions (41). The corresponding solution is

$$\Gamma_1^{IP} = - \int_0^\tau \int_0^1 \int_0^{\hat{\xi}} G(\hat{\xi}, \eta; \xi_1, \hat{\eta}_1; \tau - t) \phi(\xi_1, \hat{\eta}_1, t) d\hat{\eta} d\xi dt, \tag{45}$$

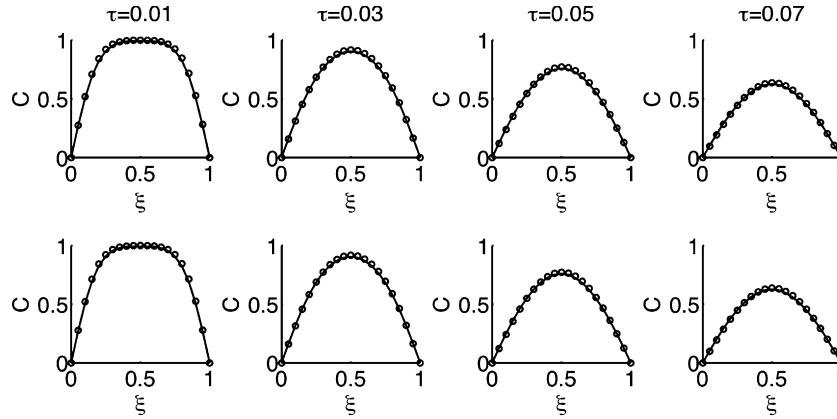


Fig. 4. Temporal snapshots of contaminant concentration distributions at two heights ($\eta = 0.1$ and $\eta = 0.4$ across the width of the aquifer provided by the perturbation (solid line) and numerical (dots) solutions of the natural attenuation problem with $\alpha = 2$ and $Pe = 0.5$.

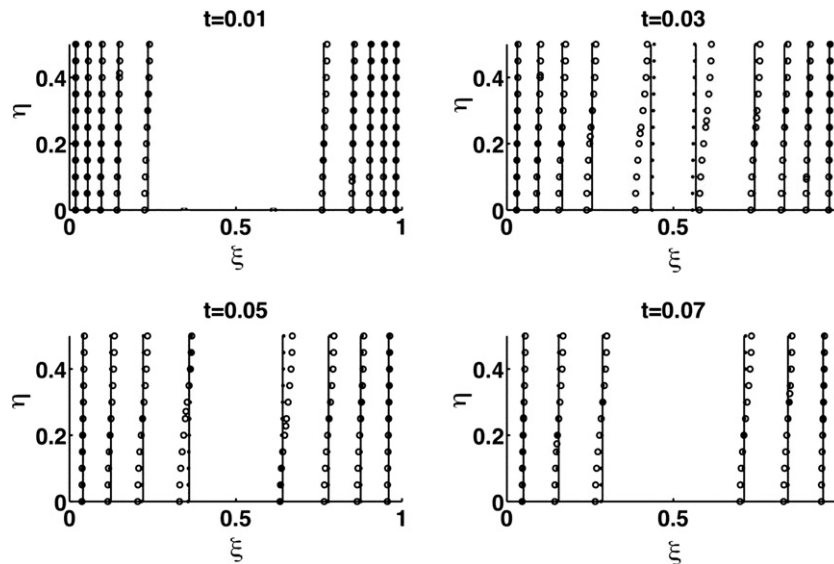


Fig. 5. Temporal snapshots of contaminant concentration distributions provided by the perturbation (solid line) solution of natural attenuation problem with $Pe = 0.5$ and $\alpha = 0$ (solid lines), $\alpha = 4.0$ (dots) and $\alpha = 20.0$ (circles).

where

$$\phi(\xi, \hat{\eta}, \tau) = - \left[U_1(\xi, \hat{\eta}) \frac{\partial \Gamma_0^{IP}}{\partial \xi}(\xi, \hat{\eta}) + V_1(\xi, \hat{\eta}) \beta^{\frac{1}{2}} \frac{\partial \Gamma_0^{IP}}{\partial \eta}(\xi, \hat{\eta}) \right] \times e^{-\frac{\beta \tau}{2}(\xi - \frac{1}{2})} \quad (46)$$

The integrals in (45) were evaluated both analytically and numerically, with the two approaches leading to the identical results.

Fig. 6 shows the steady-state contaminant distributions corresponding to three alternative spill locations, three values of α and two values of $\beta = D_T/D_L$. (Recall that $\alpha = 0$ corresponds to the fully decoupled flow model, and that the influence of the seawater boundary on flow and transport patterns increases with the value of α .) Regardless of the location of the spill, the value of α affects the contaminant concentration along the seaward (right) boundary. Its influence diminishes with the distance from the sea.

An important feature of both the natural attenuation and point spill problems is that as α increases the contaminant concentration decreases in the lower right section of the aquifer and increases in its upper right section. This is evident in both the isotropic and anisotropic cases. This behavior appears to be a universal characteristic of contaminant transport in coastal aquifers that reflects the dominant flow patterns. At the bottom of the seaward boundary there is an influx of uncontaminated (salty) water, which causes the decrease in contaminant in that region of the aquifer. However, this intruding sea water diverts the freshwater flow inside the aquifer upwards, thus causing the increase in concentration at the upper seaward boundary.

This general finding about the influence of the sea boundary – the elevated concentrations in the upper seaward regions of coastal aquifer – remains valid for aquifer systems that are more realistic than the one conceptualized

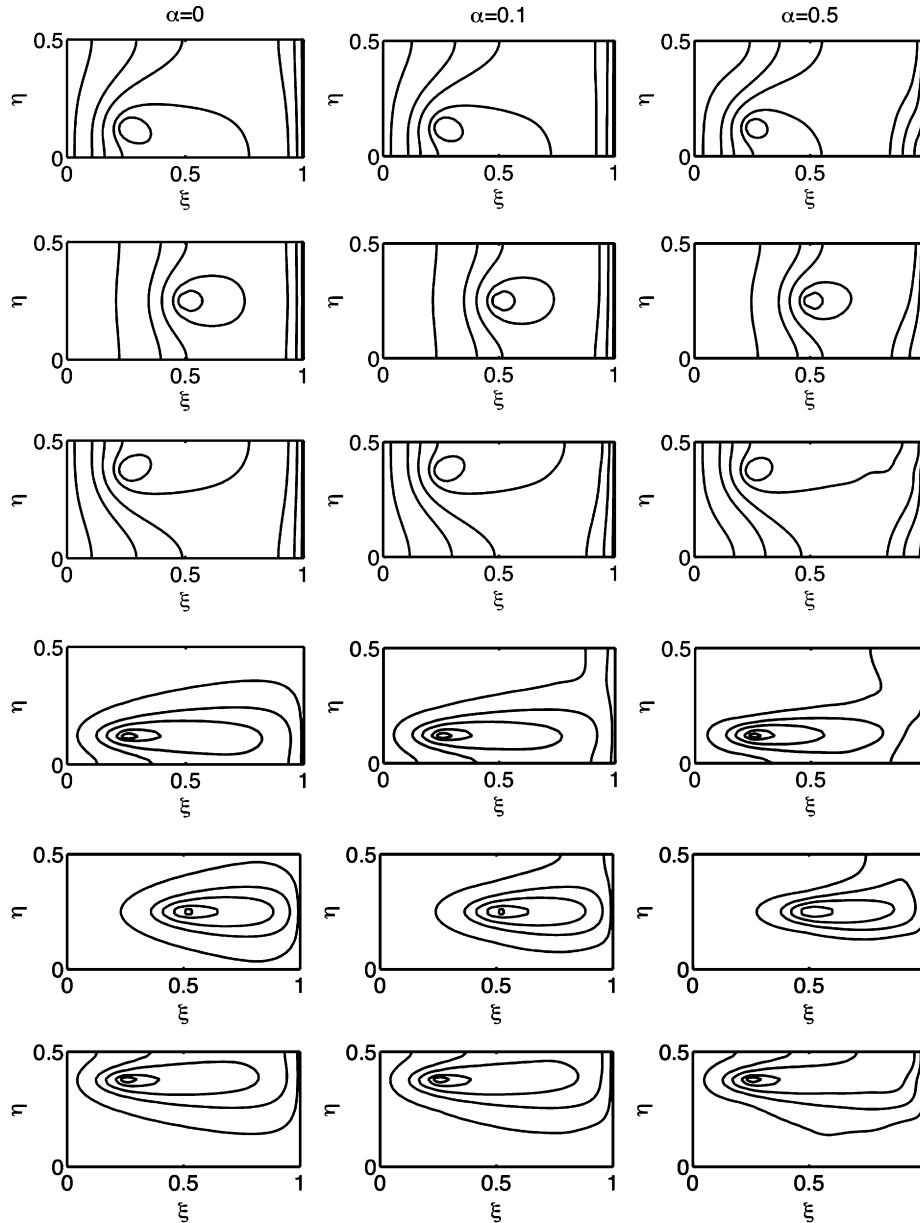


Fig. 6. Concentration isolines corresponding to three locations of the spill, three values of the coupling parameter α and two values of the anisotropy ratio β . The top three rows correspond to $\beta = 1$ and the bottom three are for $\beta = 0.1$. From top to bottom, the three spill locations (ζ, η) are at $(0.25, 0.125)$, $(0.5, 0.5)$ and $(0.25, 0.375)$, respectively.

by Henry’s problem, including the aquifer system depicted in Fig. 1. For example, it helps to explain the higher than expected contaminant concentrations in the surf zone observed by Boehm et al. [2,3], and crop failures in the fields that are adjacent to the sea and are irrigated with (contaminated) water from unconfined aquifers.

5.2. Small Péclet number

A solution of the contaminant transport problem (40)–(41) can be represented by expansion (35). The leading term in this expansion satisfies

$$\frac{\partial \Gamma_0^{SP}}{\partial \tau} = \left(\frac{\partial^2 \Gamma_0^{SP}}{\partial \xi^2} + \beta \frac{\partial^2 \Gamma_0^{SP}}{\partial \eta^2} \right) + \delta(\xi - \zeta')\delta(\eta - \eta') \quad (47)$$

subject to the initial and boundary conditions (41). The corresponding solution is

$$\begin{aligned} \Gamma_0^{SP} = & \frac{2}{\pi^2 \zeta'} \sum_{n=1}^{\infty} \frac{1}{n^2} \sin(n\pi\xi) \sin(n\pi\zeta') (1 - e^{-\pi^2 n^2 t}) \\ & + \frac{4}{\pi^2 \zeta'} \sum_{n,m=1}^{\infty} \frac{n^2}{n^2 + m^2 / \zeta'^2} \cos(n\pi\xi) \sin(n\pi\zeta') \\ & \times \cos\left(\frac{m\pi\eta}{\zeta}\right) \cos\left(\frac{m\pi\eta'}{\zeta}\right) \left[1 - e^{-\pi^2 (n^2 + \frac{m^2}{\zeta'^2}) t} \right]. \end{aligned} \quad (48)$$

The first-order term satisfies

$$\frac{\partial \Gamma_1^{SP}}{\partial \tau} = \left(\frac{\partial^2 \Gamma_1^{SP}}{\partial \xi^2} + \beta \frac{\partial^2 \Gamma_1^{SP}}{\partial \eta^2} \right) - U_0^{SP} \frac{\partial \Gamma_0^{SP}}{\partial \xi} \quad (49)$$

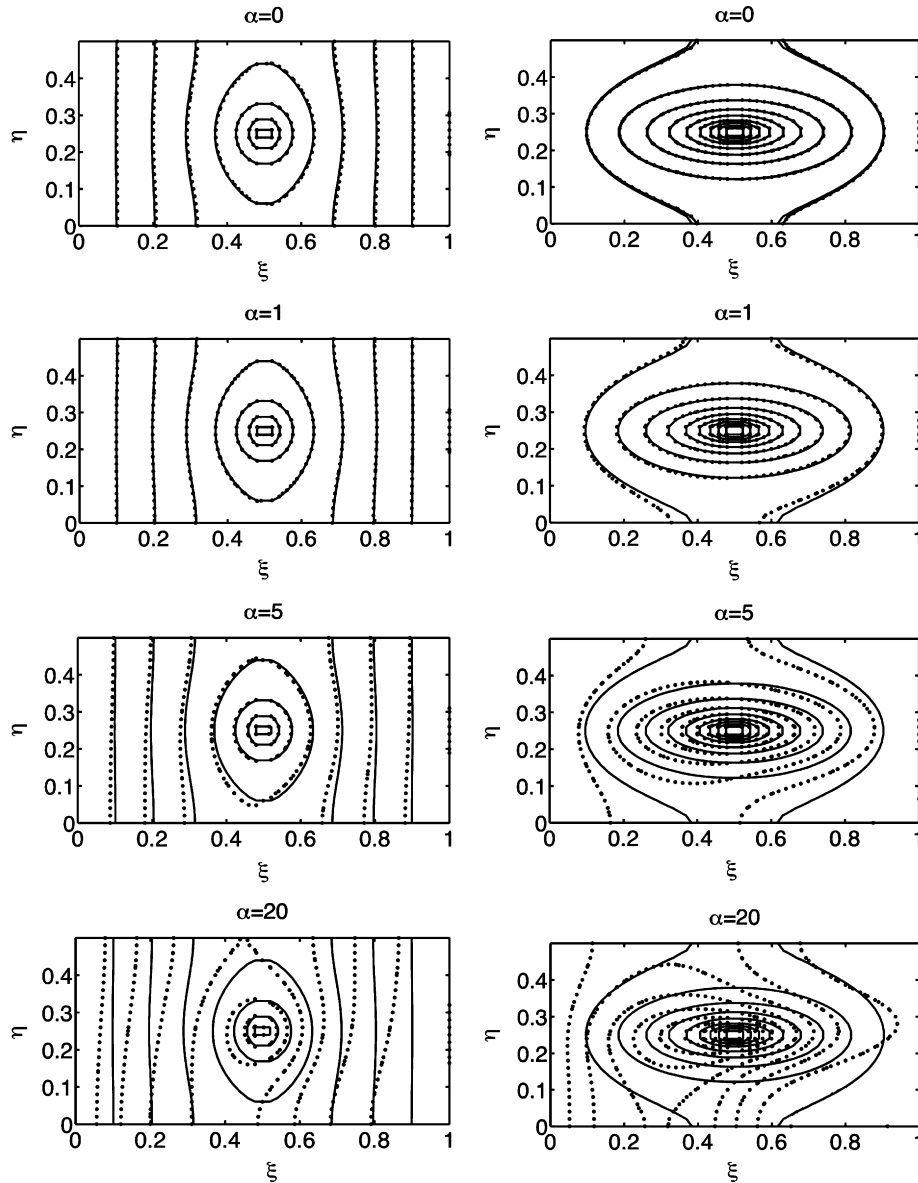


Fig. 7. Steady-state concentration isolines for a localized spill at low Péclet numbers, four values of the coupling parameter α and two values of the anisotropy coefficient (Left column is $\beta = 1$. Right column is $\beta = 0.1$). The dark lines correspond to purely diffusive transport ($Pe = 0$), and the lighter lines correspond to diffusion-dominated transport with $Pe = 0.5$.

subject to the initial and boundary conditions (41). The corresponding solution is

$$\begin{aligned}
 \Gamma_1^{\text{SP}} = & - \int_0^\tau \int_0^1 \int_0^{\hat{\xi}} G(\hat{\xi}, \eta; \xi_1, \hat{\eta}_1; \tau - t) U_0^{\text{SP}}(\xi_1, \hat{\eta}_1) \\
 & \times \frac{\partial \Gamma_0^{\text{SP}}(\xi_1, \hat{\eta}_1, \tau)}{\partial \hat{\xi}} d\hat{\eta}_1 d\xi_1 dt. \quad (50)
 \end{aligned}$$

Fig. 7 depicts the steady-state limit of the perturbation solution $\Gamma^{\text{SP}} \approx \Gamma_0^{\text{SP}} + Pe\Gamma_1^{\text{SP}}$ for $Pe = 0.5$, several values of α and two values of the anisotropy coefficient β . As in the natural attenuation problem, the sea boundary does not have significant influence on the contaminant transport, although the influence is more pronounced. This suggests that, for large times, advection plays a more

prominent role in the spread of contaminant than in its natural attenuation. However, for this effect to become noticeable, α has to be made so large as to render its practical realizability minimal. Additionally, the effects of advection are more noticeable for the anisotropic case. This is not surprising since the effect of anisotropy is to suppress dispersion in the transverse direction, thus increasing advective influence.

6. Summary and conclusions

We employed the Henry formulation and perturbation analyses to derive analytical solutions describing contaminant migration in coastal aquifers. We showed that flow and transport in coastal aquifers can be characterized by

two dimensionless parameters, the Péclet number Pe and a coupling parameter α . The former compares advective and dispersive mechanisms of transport, while the latter quantifies the density effects and the influence of the saltwater boundary on the flow field. The analytical solutions derived describe natural attenuation of, and contaminant spill in, coastal aquifers for intermediate and low Péclet numbers. Our analysis leads to the following major conclusions.

- (1) The saltwater boundary significantly affects contaminant transport in the intermediate Péclet number (advection-diffusion) regime. Its influence on transport in the small Péclet number (diffusion dominated) regime is significantly smaller. This is to be expected, since the main effect of the saltwater boundary is to modify the velocity field, i.e., the advective mechanism of transport.
- (2) For the sea boundary to affect transport patterns in the low Péclet number regime, the coupling parameter α must be very large. For real coastal aquifers it is highly unlikely that this situation will occur.
- (3) Although the Henry formulation is a simplified model of coastal aquifers, it provides a useful physical insight into transport mechanisms affecting the spread of contaminants in such systems. The saltwater intrusion forces contaminant transport towards the upper seaward boundary, thus causing elevated contaminant discharge into the surf zone at beach areas.
- (4) Our analytical solutions also provide insight for management decisions that must be made regarding the use of coastal aquifers for irrigation and drinking water purposes. In particular, they can provide guidelines for the viability of natural attenuation of contaminated coastal aquifers after the sources of contamination have been eliminated.

References

- [1] Vengosh A, Weintal E, Kloppmann E. The BOREMED team. Natural boron contamination in mediterranean groundwater. *Geotimes* 2004(May):20–5.
- [2] Boehm A, Shellenbarger G, Paytan A. Groundwater discharge: potential association with fecal indicator bacteria in the surf zone. *Environ Sci Technol* 2004;38(13):3558–66.
- [3] Boehm A, Paytan A, Shellenbarger G, Davis K. Composition and flux of groundwater from a california beach aquifer: Implications for nutrient supply to the surf zone. *Cont Shelf Res* 2006;26: 269–82.
- [4] Tartakovsky DM, Federico VD. An analytical solution for contaminant transport in non-uniform flow. *Transport Porous Med* 1997;27(1):85–97.
- [5] Bear J, Dagan G. Some exact solutions of interface problems by means of the hodograph method. *J Geophys Res* 1964;69:1563–72.
- [6] Huppert HE, Woods AW. Gravity-driven flows in porous layers. *J Fluid Mech* 1995;292:55–69.
- [7] Naji A, Cheng AH-D, Ouazar D. Analytical stochastic solutions of saltwater/freshwater interface in coastal aquifers. *Stoch Hydrol Hydraul* 1998;12:413–29.
- [8] Kacimov AR, Obnosov YV. Analytical solution for a sharp interface problem in sea water intrusion into a coastal aquifer. *Proc Royal Soc Lond A* 2001;457(2016):3023–38.
- [9] Henry HR. Effects of dispersion on salt encroachment in coastal aquifers. Technical Report on Water Supply, Paper 1613-C, US Geological Survey; 1964.
- [10] Simpson MJ, Clement TP. Theoretical analysis of the worthiness of Henry and elder problems as benchmarks of density-dependent groundwater flow models. *Adv Water Resour* 2003;26(1):17–31.
- [11] Dentz M, Tartakovsky DM, Abarca E, Guadagnini A, Sanchez-Vila X, Carrera J. Variable density flow in porous media. *J Fluid Mech* 2006;561:209–35.
- [12] Kalejaiye BO, Cardoso SSS. Specification of the dispersion coefficient in the modeling of gravity-driven flow in porous media. *Water Resour Res* 2005;41.
- [13] Hunt G, Kaye N. Pollutant flushing with natural displacement ventilation. *Building Environ* 2006;41(9):1190–7.
- [14] Bolster DT, Linden PF. Contaminated ventilated filling boxes. *J Fluid Mech*; under review.